

# SUPPORTING INFORMATION

## High-Temperature Reversible Martensitic Transition in an Excited-State

### Intramolecular Proton Transfer Fluorophore

*Fabio Borbone,<sup>\*,†</sup> Angela Tuzi,<sup>†</sup> Antonio Carella,<sup>†</sup> Domenica Marabello,<sup>‡</sup> Stefano Luigi Oscurato,<sup>§</sup> Stefano Lettieri,<sup>+</sup> Pasqualino Maddalena<sup>§</sup> and Roberto Centore<sup>†</sup>*

<sup>†</sup> Department of Chemical Sciences, University of Napoli Federico II, Via Cintia, 80126 Napoli, Italy

<sup>‡</sup> Department of Chemistry, University of Torino, Via Verdi 8, 10124 Torino, Italy; CRISDI, Interdepartmental center for Crystallography, University of Torino, Italy

<sup>§</sup> Department of Physics E. Pancini, University of Napoli Federico II, Via Cintia, 80126 Napoli, Italy

<sup>+</sup>Institute of Applied Sciences and Intelligent Systems, National Research Council (ISASI-CNR), Via Campi Flegrei 34, 80078 Pozzuoli (NA), Italy

\*Email: fabio.borbone@unina.it

#### Contents:

- Experimental section
- Scheme S1 reporting the synthesis scheme of **DBOX**.
- Figure S1 reporting DSC diagram of **DBOX-I** at several scan rates.
- Figure S2 reporting calculated and experimental PXRD spectra of **DBOX-I**.
- Figure S3 reporting a comparison of transition bands at POM and orientation of molecules.
- Figures S4, S5, S6 and S7 reporting the ORTEP view molecules in phases I, II and III of **DBOX**.
- Figure S8 reporting the overlay of **DBOX-I** and **DBOX-III** molecules.
- Table S1 reporting crystal, collection and refinement data for phases I, II and III of **DBOX**.
- Figure S9 reporting the molecular packing of **DBOX-II**.
- Figure S10 reporting the lateral displacement of dimers in **DBOX-I** and **DBOX-II**.
- Figure S11 reporting C-H...S contacts in **DBOX-I** and **DBOX-II**.
- Figure S12 reporting the Hirshfeld fingerprint plots of **DBOX-I**, **DBOX-II** and **DBOX-III**.
- Figure S13 reporting the absorption spectra of **DBOX** in several solvents.
- Figure S14 reporting the scheme of ES IPT emission.
- Figure S15 reporting emission spectra of **DBOX** at several excitation wavelengths.
- Figure S16 reporting time-resolved photoluminescence spectra.

## EXPERIMENTAL SECTION

Ethyl benzothiazole-2-carboxylate and 3-diethylaminophenol were commercially available (Sigma-Aldrich) and used without further purification. Optical observations were performed by using a Zeiss Axioscop polarizing microscope equipped with a FP90 Mettler heating stage (the internal factory calibration was checked with benzoic acid and caffeine standards, accuracy  $\pm 0.6$  °C). DSC thermograms were recorded using a Perkin Elmer Pyris 1 under nitrogen flow (20 mL/min) on a mass of sample of about 5 mg. The temperature and heat flow scales were calibrated with an indium 99.999% standard at the different heating rates used (1 and 10 °C/min).  $^1\text{H}$  and  $^{13}\text{C}$  NMR spectra were recorded using a Varian Inova 500 spectrometer operating at 500 MHz. UV-Visible and fluorescence spectra were recorded with JASCO V-560 and FP-750 spectrometers.

**Synthesis of DBOX.** 4-Diethylaminosalicylic acid was prepared by adding 3-diethylaminophenol (16.5 g, 100 mmol) and  $\text{KHCO}_3$  (20.0 g, 200 mmol) to 30.0 g glycerol, heating to 140 °C and bubbling finely dispersed  $\text{CO}_2$ . After 20 h the liquid was cooled and diluted with 100 mL water. The unreacted product was filtered off and HCl was added to lower pH. During addition more unreacted product was precipitated and filtered off. At pH of about 4.5 pure 4-diethylaminosalicylic (2.60 g, yield: 12.4%) was precipitated, filtered and used without further purification.

**DBOX.** Ethyl benzothiazole-2-carboxylate was converted to ethyl benzothiazole-2-carbohydrazide by refluxing in ethanol with excess hydrazine. Ethyl benzothiazole-2-carbohydrazide (1.23 g, 6.37 mmol) and 4-diethylaminosalicylic acid (1.40 g, 6.68 mmol) were grinded and slowly added to 75 g polyphosphoric acid at 200 °C under stirring. The mixture was stirred at 150 °C overnight, added with 150 mL iced water and cooled in an ice bath. A solution of 69 g KOH in 100 mL water was cooled in freezer and slowly added, by keeping the temperature between 20 and 30 °C. The precipitate was filtered, washed with water, dried and purified by chromatography (Silica, DCM-DCM/acetone) to give 1.25 g of pure product. Yield: 54 %.  $^1\text{H}$ -NMR ( $\text{CHCl}_3$ -*d*):  $\delta$  1.25 (t, 6H);  $\delta$  3.45 (m, 4H);  $\delta$  6.56 (s, 1H);  $\delta$  6.65 (d, 1H);  $\delta$  7.60 (m, 2H);  $\delta$  7.88 (d, 1H);  $\delta$  8.03 (m, 1H);  $\delta$  8.26 (m, 1H);  $\delta$  10.08 (s, 1H).  $^{13}\text{C}$ -NMR ( $\text{CHCl}_3$ -*d*):  $\delta$  12.15, 31.07, 122.11, 124.80, 125.20, 127.50, 127.60, 127.87, 128.87, 135.56, 135.96, 149.63, 153.51, 153.64, 159.83, 161.27, 207.13.

**X Ray diffraction analysis.** Single crystals of phase I suitable for X-ray structural analysis were obtained by slow evaporation from heptane solution at room temperature. Single crystals of phase III suitable for X-ray diffraction were successfully grown by diffusion of **DBOX** vapors on a target of phase III powder. In particular, a small amount of **DBOX** was placed in a Pasteur pipette, near the large opening, and the pipette was placed horizontally on a heating plate. The compound was melted

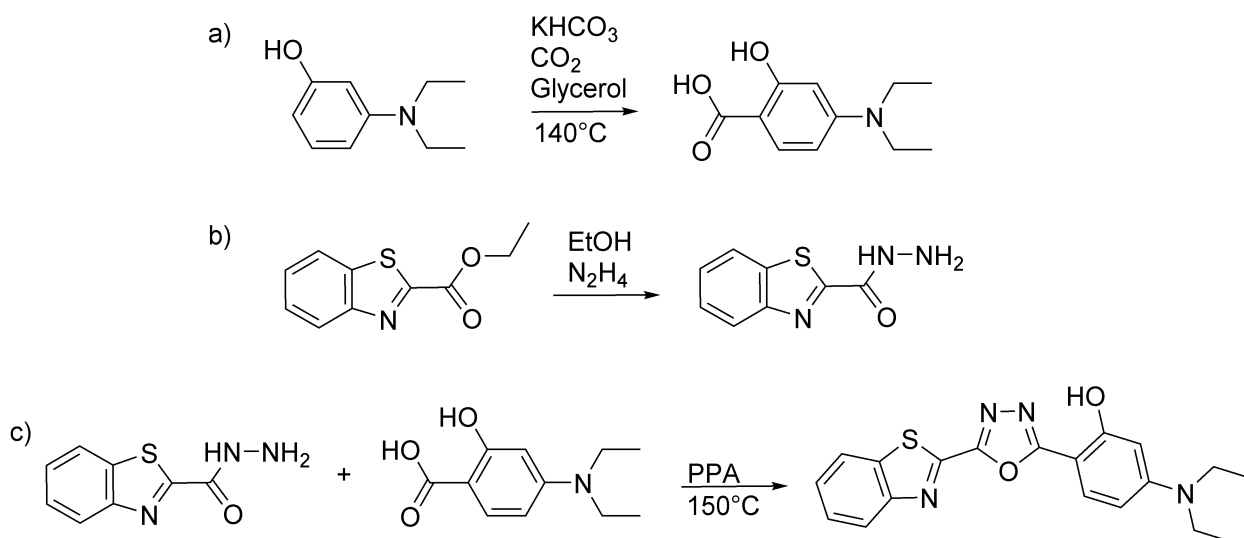
and kept at about 200 °C under a gentle nitrogen flow. A glass slide covered with phase III powder was placed few millimeters far from the opening, facing the vapor flow. The opening of the pipette was placed near the edge of the hot plate, so that the target did not heat up. After few hours, single crystals of phase III grew on top of the powder. One selected crystal of each compound was mounted in flowing N<sub>2</sub> at -100 °C on a Bruker-Nonius KappaCCD diffractometer equipped with Oxford Cryostream apparatus (graphite monochromated MoK $\alpha$  radiation,  $\lambda = 0.71073 \text{ \AA}$ , CCD rotation images, thick slices,  $\varphi$  and  $\omega$  scans to fill asymmetric unit). Data collection on **DBOX-I** crystal was also performed at ambient temperature to confirm that no further thermal events occur on cooling to -100 °C. Reduction of data and semiempirical absorption correction were done using SADABS program. The structures were solved by direct methods (SIR97 program)<sup>1</sup> and refined by the full-matrix least-squares method on  $F^2$  using SHELXL-2016 program<sup>2</sup> with the aid of the program WinGX.<sup>3</sup> H atoms bonded to C were generated stereochemically and refined by the riding model, those bonded to O were found in difference Fourier maps and their coordinates were refined. For all H atoms,  $U_{\text{iso}}(\text{H})$  equal to 1.2 $U_{\text{eq}}$  or 1.5 $U_{\text{eq}}$  ( $C_{\text{methyl}}$ ) of the carrier atom was used.

Single crystal X-ray data collection of phase II at 180 °C was performed on a Xcalibur, AtlasS2, Gemini Ultra diffractometer equipped with a nitrogen Oxford Diffraction CryojetHT device. The crystal was kept at 180(2) °C during data collection and exhibited slightly high temperature damages at the end of data collection, so that during integration with CrysAlisPro<sup>4</sup> a correction for crystal decay was applied. The crystal was heated through a nitrogen flux from room to 180 °C in about 30 minutes. Since the crystal sublimates with a long exposure under warm nitrogen flux, during data collection it was maintained at 180 °C for only one hour, setting a fast exposure time for images and thus giving up on the accuracy of structure determination. At the end of data collection, the crystal looks unaltered and data collected were enough to resolve the structure. Using Olex2,<sup>5</sup> the structure was solved with the ShelXT<sup>6</sup> structure solution program using Intrinsic Phasing and refined with the ShelXL<sup>2</sup> refinement package using Least Squares minimisation. In the case of phase II, one of the two ethyl groups is disordered over two sites. The two split positions were refined introducing some restraints on bond lengths and thermal parameters (SADI and ISOR instructions of SHELXL). The final refined occupancy factors of the split positions are 0.57(2) and 0.43(2). All atoms but hydrogens were localized in E-maps or Fourier maps and anisotropically refined, although thermal factors show very high values, as expected due to the high temperature of data collection. H atoms bonded to C atoms were placed in calculated positions and refined with the riding model. The H atom bonded to O was found in a difmap and its coordinates were refined with some restraints on the bond length. For all H atoms,  $U_{\text{iso}} = 1.2$  or 1.5 times  $U_{\text{eq}}$  of the carrier atom. For the cell determination at

temperature values from 20 to 190 °C, a new single crystal of **DBOX** was heated under nitrogen flow at steps of 10 degrees, allowing the stabilization of the temperature at each step.

Crystal data and structure refinement details are reported in Table S1. The figures were generated using ORTEP-3 and Mercury CSD 3.3 programs.<sup>7</sup> Fingerprint plot analysis was performed using the program CrystalExplorer.<sup>8</sup> All crystal data were deposited at Cambridge Crystallographic Data Centre with assigned number CCDC 1942324 (**DBOX-I**), 1942325 (**DBOX-II**), 1942326 (**DBOX-III**) and 1952840 (**DBOX-I-RT**). These data can be obtained free of charge from [www.ccdc.cam.ac.uk/data\\_request/cif](http://www.ccdc.cam.ac.uk/data_request/cif).

**Time-resolved photoluminescence.** Time-resolved photoluminescence measurements were performed using a frequency-tripled mode-locked Nd:YAG laser as excitation source (355 nm wavelength, 20 ps time duration of laser pulses). The laser pulses were slightly focused (~ 5 mm spot) at the free surface of a **DBOX**/solvent solution gathered in a glass capsule. The fluorescence signal was collected by a confocal lens system and imaged on the input slit of a monochromator equipped with 150 grooves/mm grating, coupled with a streak camera. Each acquisition was obtained by integration over 1000 laser pulses. The experimental uncertainty of the overall system on time measurements was about 0.1 ns.



**Scheme S1.** Synthesis scheme of 4-diethylaminosalicylic acid (a), ethyl benzothiazole-2-carbohydrazide (b) and **DBOX** (c).

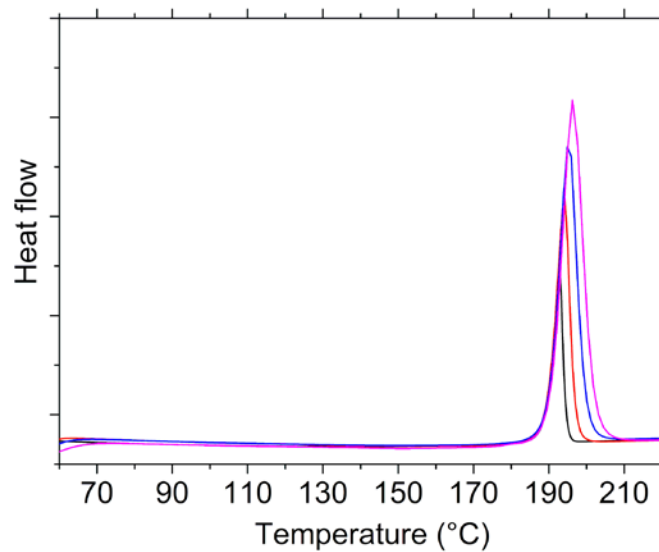


**Figure S1.** DSC diagram of **DBOX-I** powder recorded at 20 °C/min (black line), 40 °C/min (red line), 60 °C/min (blue line) and 80 °C/min (magenta line).

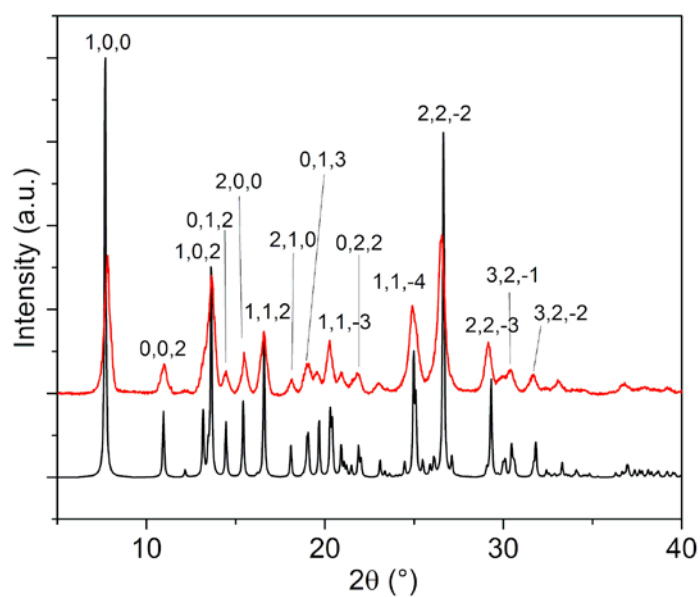


**Figure S2.** Calculated (black line) and experimental (red line) PXRD spectra of **DBOX-I** with indexing of reflections.

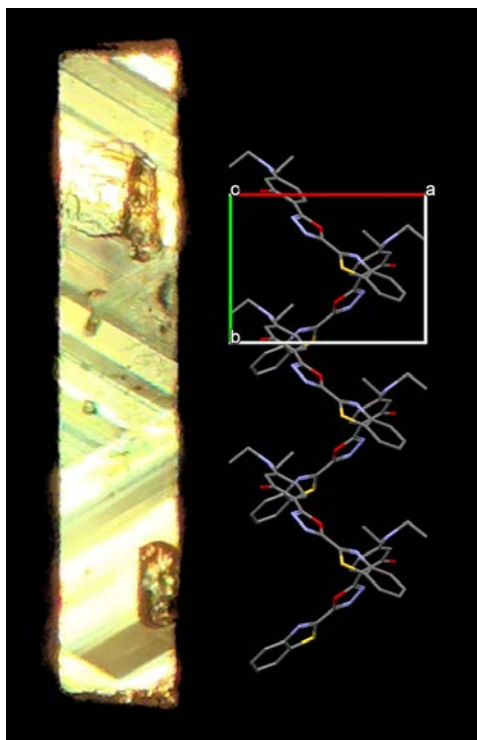


**Figure S3.** Photograph of a **DBOX** single crystal during the II→I transition and comparison with the orientation of molecules in the crystal lattice of phase II.

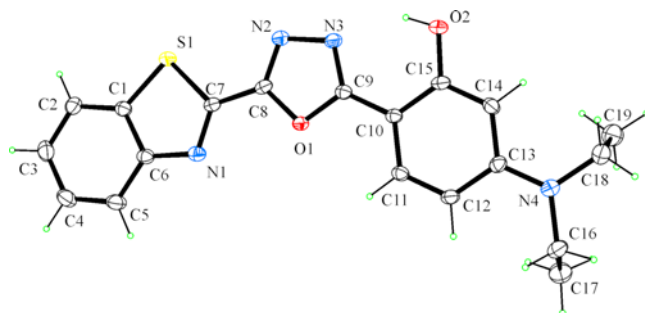


**Figure S4.** Ortep view of **DBOX-I** ( $T = -100\text{ }^{\circ}\text{C}$ ) with ellipsoids drawn at 30% probability level.

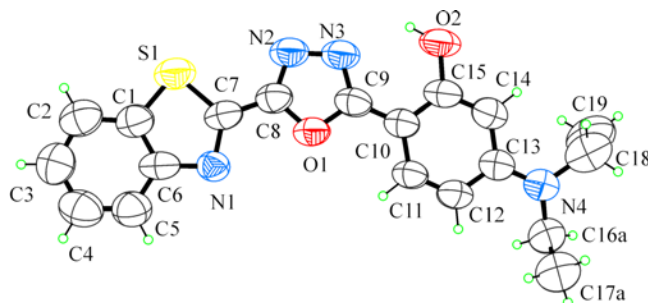


**Figure S5.** Ortep view of **DBOX-II** ( $T = 180\text{ }^{\circ}\text{C}$ ) with ellipsoids drawn at 30% probability level.

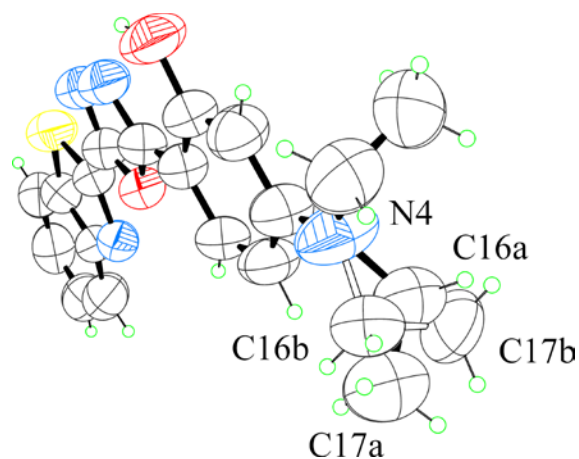


**Figure S6.** Ortep view of **DBOX-II** ( $T = 180\text{ }^{\circ}\text{C}$ ) showing the two split positions of one N-ethyl group. Thermal ellipsoids are drawn at 30 % probability level.

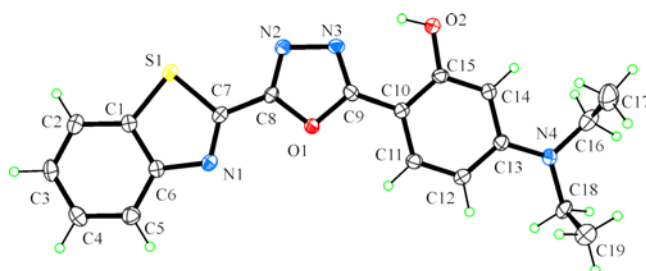


**Figure S7.** Ortep view of **DBOX-III** ( $T = -100\text{ }^{\circ}\text{C}$ ) with ellipsoids drawn at 30 % probability level.

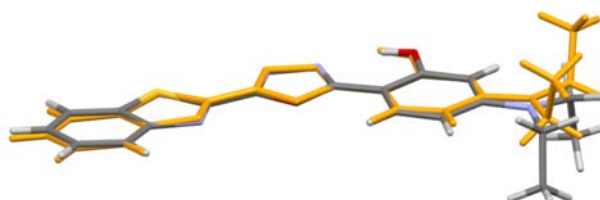


**Figure S8.** Overlay of **DBOX-I** and **DBOX-III**.

**Table S1.** Crystal data and structure refinement details for phase I, II and III of **DBOX**.

	<b>DBOX-I</b>	<b>DBOX-I-RT</b>	<b>DBOX-II</b>	<b>DBOX-III</b>
CCDC number	1942324	1952840	1942325	1942326
Empirical formula	C <sub>19</sub> H <sub>18</sub> N <sub>4</sub> O <sub>2</sub> S	C <sub>19</sub> H <sub>18</sub> N <sub>4</sub> O <sub>2</sub> S	C <sub>19</sub> H <sub>18</sub> N <sub>4</sub> O <sub>2</sub> S	C <sub>19</sub> H <sub>18</sub> N <sub>4</sub> O <sub>2</sub> S
Formula weight	366.44	366.44	366.44	366.44
T (K)	173(2)	298(2)	453(2)	173(2)
$\lambda$ (Å)	0.71073	0.71073	1.54184	0.71073
Crystal system	Monoclinic	Monoclinic	Monoclinic	Orthorhombic
Space group	<i>P2<sub>1</sub>/c</i>	<i>P2<sub>1</sub>/c</i>	<i>P2<sub>1</sub>/c</i>	<i>P2<sub>1</sub>2<sub>1</sub>2<sub>1</sub></i>
<i>a</i> (Å)	11.4910(12)	11.5192(14)	11.8407(18)	5.0180(17)
<i>b</i> (Å)	9.3920(18)	9.4616(3)	8.911(2)	12.632(3)
<i>c</i> (Å)	16.142(4)	16.2598(16)	17.509(3)	27.402(8)
<i>a</i> (°)	90	90	90	90
$\beta$ (°)	92.044(13)	91.970(8)	97.320(13)	90
$\gamma$ (°)	90	90	90	90
V (Å <sup>3</sup> )	1741.0(6)	1771.1(3)	1832.4(6)	1736.9(9)
Z	4	4	4	4
D <sub>calc</sub> (Mg/m <sup>3</sup> )	1.398	1.374	1.336	1.401
$\mu$ (mm <sup>-1</sup> )	0.208	0.204	1.744	0.208
F(000)	768	768	768	768
$\theta$ range (°)	2.51 - 28.50	2.79 - 27.50	3.764-67.378	2.974 - 25.010
Reflections collected / unique [R(int)]	12989 / 4248 [0.0325]	10581 / 3894 [0.0367]	11111/3210 [0.0394]	8284 / 2910 [0.0767]
Data/restraints/parameters	4248 / 0 / 240	3894 / 0 / 240	3210/22/256	2910 / 0 / 240
Goodness-of-fit on F <sup>2</sup>	1.059	1.054	1.063	1.078
Final <i>RI</i> , <i>wR2</i> indices [I>2 $\sigma$ (I)]	0.0500, 0.1182	0.0599, 0.1376	0.0824, 0.2496	0.0553, 0.1075
Final <i>RI</i> , <i>wR2</i> indices (all data)	0.0850, 0.1365	0.1125, 0.1665	0.1451, 0.3368	0.1026, 0.1271
Largest diff. peak / hole (eÅ <sup>-3</sup> )	0.404/-0.269	0.458 /-0.234	0.194/-0.306	0.623/ -0.258

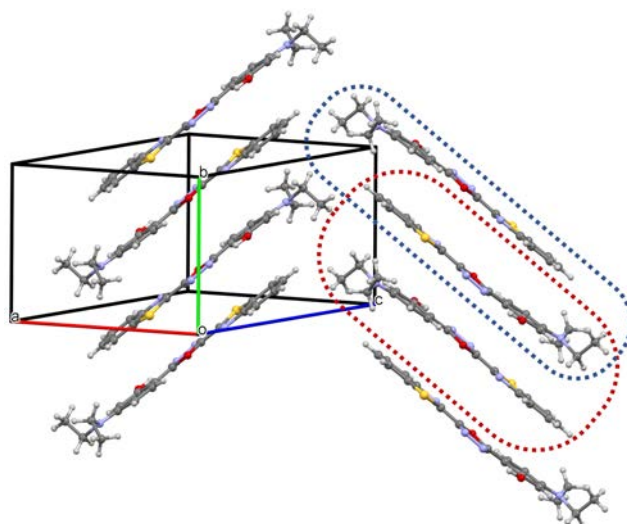


**Figure S9.** Molecular packing of **DBOX-II** with highlight of hooked (blue dotted line) and unhooked (red dotted line) dimers.

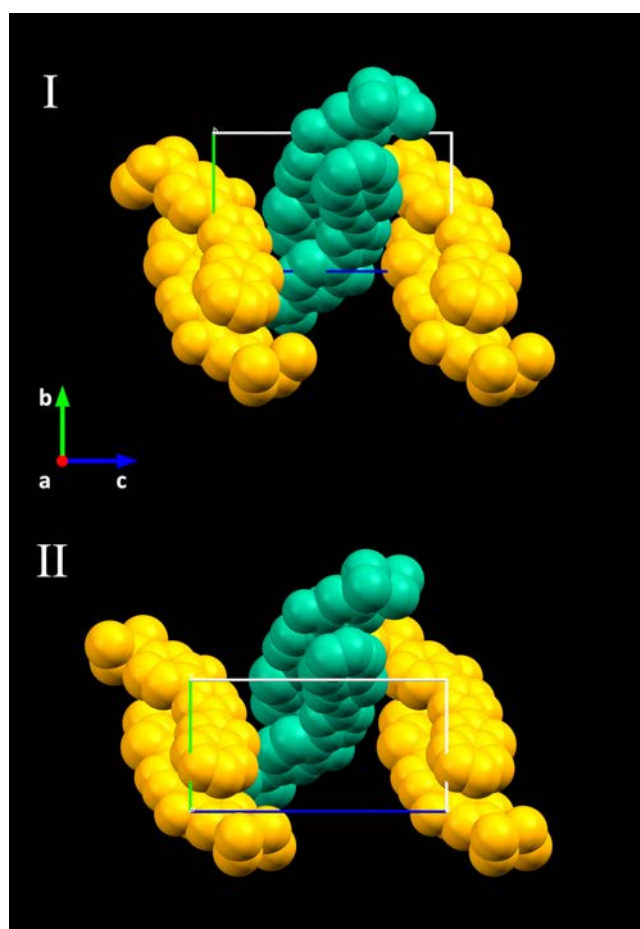


**Figure S10.** Lateral displacement of adjacent dimers in **DBOX-I** and **DBOX-II** (view along [100] direction).

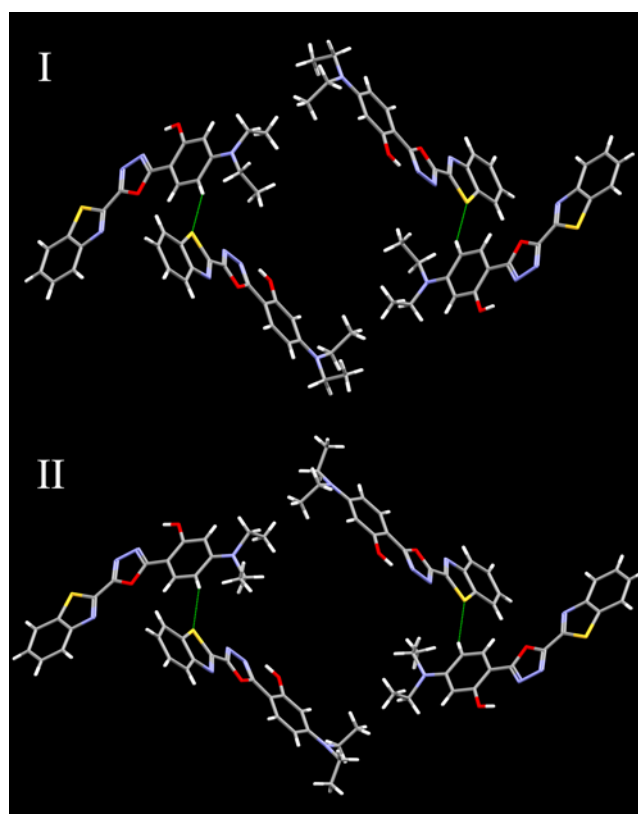


**Figure S11.** C-H...S contacts in **DBOX-I** and **DBOX-II**.

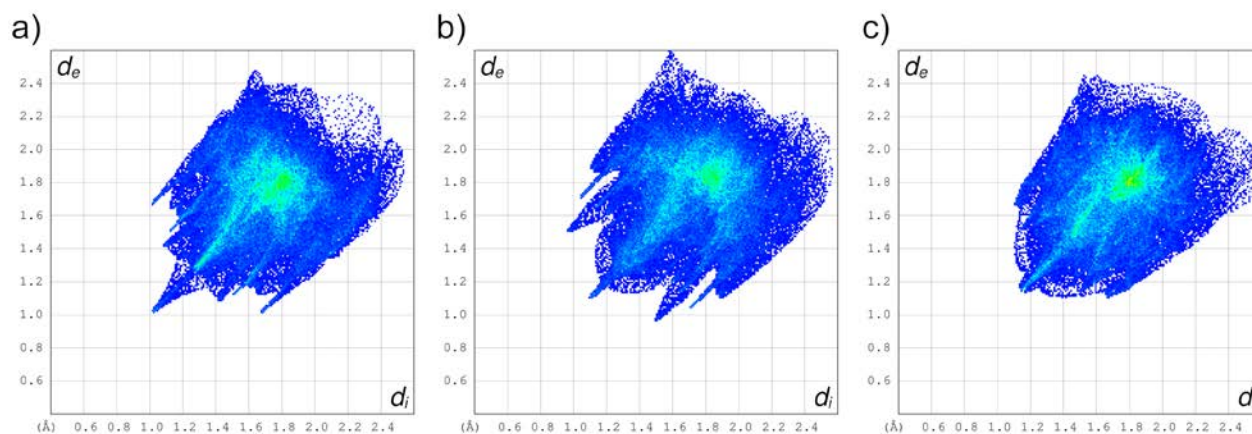


**Figure S12.** Hirshfeld fingerprint plots of **DBOX-I** (a), **DBOX-II** (b) and **DBOX-III** (c). In all the three phases there is a predominance of parallel face-to-face contacts between translated molecules, as shown by the green areas centered at  $d_i + d_e = 3.6 \text{ \AA}$ . External wings and spikes in phase I and II are mainly due to C-H...S contacts. Phase II is characterized by evident spikes at  $(d_i, d_e) = (1.0, 1.5)$  and  $(d_i, d_e) = (1.5, 1.0)$  corresponding to C-H...N interactions involving mainly the nitrogen of the benzothiazole moiety and ethyl chains.

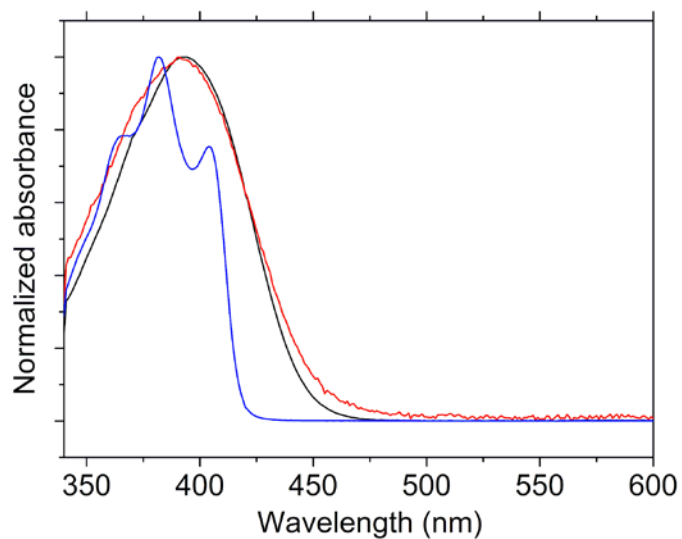


**Figure S13.** Absorption spectra of **DBOX** in heptane (blue line), dichloromethane (black line) and dimethylsulfoxide (red line).

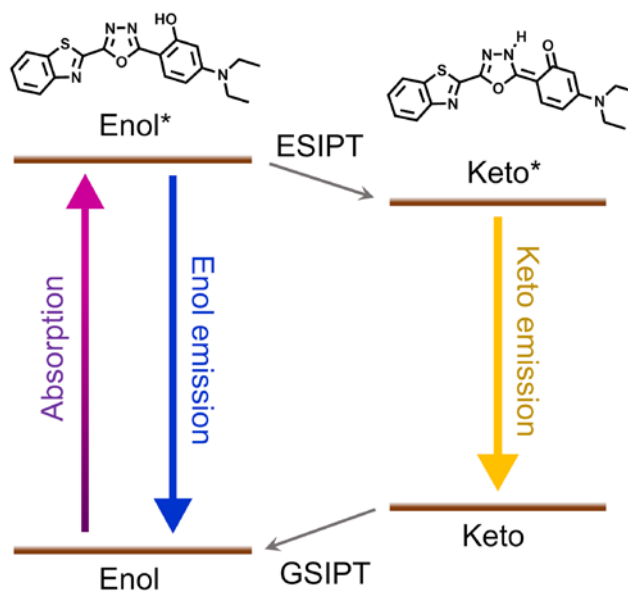


**Figure S14.** Scheme of the emission from enol and keto forms in the excited-state intramolecular proton transfer process.

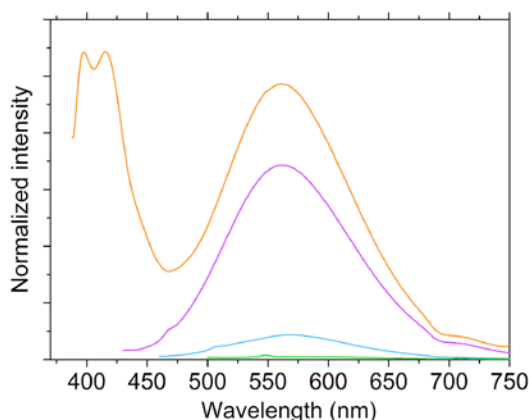


**Figure S15.** Emission spectra of **DBOX** in 2:1 isopropanol/methoxyethanol excited at 380 nm (orange line), 410 nm (purple line), 440 nm (blue line) and 470 nm (green line).

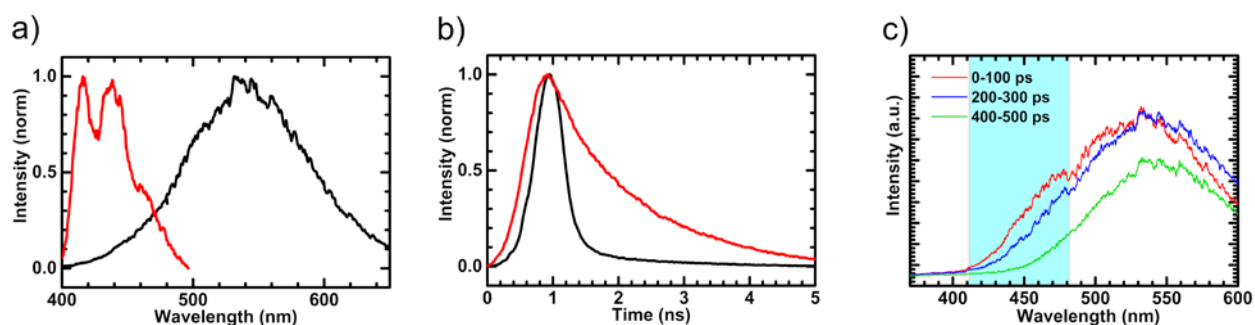


**Figure S16.** Time-integrated fluorescence spectra (a) for **DBOX** in decane (red line) and in t-butanol (black line). Fluorescence decay of **DBOX** in t-butanol (b) at 450 nm (black line) and 550 nm (red line). Time-resolved fluorescence spectra of **DBOX** in t-butanol (c). Emission decay in decane is found to be spectrally uniform, i.e. the different wavelength component of the fluorescence emission exhibit very similar decay rates. A single-exponential fit gives a lifetime of 1.8 ns for the enol tautomer at 450 nm. **DBOX** in t-butanol shows keto emission at about 550 nm with a small contribution of the enol form at 450 nm. These two components show different kinetics. The decay of the 450 nm component is significantly faster than the one observed for the 550 nm peak. More in detail, the blue emission decays accordingly to a double exponential kinetics (b), with a fast and dominant component (96%) of lifetime  $\tau_1 = 0.2$  ns and a slower component (4%) of lifetime  $\tau_2 = 1.7$  ns (black line). This behavior is consistent with an expected rapid decay of the enol emission in the protic solvent due to the fast proton transfer, which can be appreciated in the transient emission spectra (c), although limited by the instrumental resolution. On the other hand, the decay of the 550 nm keto peak can be fitted adequately via a single-exponential function of longer lifetime 1.3 ns (b, red line).

## REFERENCES

- (1) Altomare, A.; Burla, M. C.; Camalli, M.; Cascarano, G. L.; Giacovazzo, C.; Guagliardi, A.; Moliterni, A. G. G.; Polidori, G.; Spagna, R. SIR 97: A New Tool for Crystal Structure Determination and Refinement. *J. Appl. Crystallogr.* **1999**, *32*, 115–119.
- (2) Sheldrick, G. M. Crystal Structure Refinement with SHELXL. *Acta Crystallogr. Sect. C Struct. Chem.* **2015**, *71*, 3–8.
- (3) Farrugia, L. J. WinGX and ORTEP for Windows : An Update. *J. Appl. Crystallogr.* **2012**, *45*, 849–854.
- (4) CrysAlisPro 1.171.39.46 (Rigaku Oxford Diffraction, 2018).
- (5) Dolomanov, O. V.; Bourhis, L. J.; Gildea, R. J.; Howard, J. A. K.; Puschmann, H. OLEX2: A Complete Structure Solution, Refinement and Analysis Program. *J. Appl. Crystallogr.* **2009**, *42*, 339–341.
- (6) Sheldrick, G. M. SHELXT - Integrated Space-Group and Crystal-Structure Determination. *Acta Crystallogr. Sect. A Found. Crystallogr.* **2015**, *71*, 3–8.
- (7) Macrae, C. F.; Bruno, I. J.; Chisholm, J. A.; Edgington, P. R.; McCabe, P.; Pidcock, E.; Rodriguez-Monge, L.; Taylor, R.; van de Streek, J.; Wood, P. A. Mercury CSD 2.0 – New Features for the Visualization and Investigation of Crystal Structures. *J. Appl. Crystallogr.* **2008**, *41*, 466–470.
- (8) Spackman, M. A.; McKinnon, J. J. Fingerprinting Intermolecular Interactions in Molecular Crystals. *CrystEngComm* **2002**, *4*, 378–392.